isvr Institute of Sound and Vibration Research

BOMBARDIER Dash-8 Q400 Fuselage Section with Five Decentralized Velocity Feedback Control Units

P. Gardonio and C. Gonzalez Diaz

ISVR Technical Memorandum No 983

January 2009

University of Southampton

SCIENTIFIC PUBLICATIONS BY THE ISVR

Technical Reports are published to promote timely dissemination of research results by ISVR personnel. This medium permits more detailed presentation than is usually acceptable for scientific journals. Responsibility for both the content and any opinions expressed rests entirely with the author(s).

Technical Memoranda are produced to enable the early or preliminary release of information by ISVR personnel where such release is deemed to the appropriate. Information contained in these memoranda may be incomplete, or form part of a continuing programme; this should be borne in mind when using or quoting from these documents.

Contract Reports are produced to record the results of scientific work carried out for sponsors, under contract. The ISVR treats these reports as confidential to sponsors and does not make them available for general circulation. Individual sponsors may, however, authorize subsequent release of the material.

SCIENTIFIC PUBLICATIONS BY THE ISVR

Technical Reports are published to promote timely dissemination of research results by ISVR personnel. This medium permits more detailed presentation than is usually acceptable for scientific journals. Responsibility for both the content and any opinions expressed rests entirely with the author(s).

Technical Memoranda are produced to enable the early or preliminary release of information by ISVR personnel where such release is deemed to the appropriate. Information contained in these memoranda may be incomplete, or form part of a continuing programme; this should be borne in mind when using or quoting from these documents.

Contract Reports are produced to record the results of scientific work carried out for sponsors, under contract. The ISVR treats these reports as confidential to sponsors and does not make them available for general circulation. Individual sponsors may, however, authorize subsequent release of the material.

UNIVERSITY OF SOUTHAMPTON

INSTITUTE OF SOUND AND VIBRATION RESEARCH

SIGNAL PROCESSING & CONTROL GROUP

BOMBARDIER Dash-8 Q400 Fuselage Section with Five Decentralised Velocity Feedback Control Units

by

Paolo Gardonio and Cristóbal González Díaz

ISVR Technical Memorandum Nº 983

January 2009

Authorised for issue by
Prof R Allen
Group Chairman

ABSTRACT

This report presents the experimental work carried out to implement decentralised velocity feedback control on a fuselage section of a Bombardier Dash-8 Q400 aircraft. Five velocity feedback control units have been mounted on the trim panel of the fuselage section in order to reduce its response and thus sound transmission and radiation. The stability of the five control units has been assessed with both the classic and generalised Nyquist criteria for a single and multiple feedback loops. Both passive and active effects produced by the five control units have been analysed with reference to the spatial response of the trim panel when the fuselage skin is excited by a shaker. The tests carried out have shown that the passive and active effects produced by the control units produce an overall reduction of vibration between 4 dB and 15 dB in the frequency range 30 to 520 Hz.

TABLE OF CONTENTS

1. INTRODUCTION

This report summarises the active control tests carried out on a BOMBARDIER Dash-8 Q400 fuselage section with trim panel which is equipped with five decentralised velocity feedback control units for the reduction of vibration and sound radiation.

The fuselage of current aircraft for civil transportation is made of an aluminium structure formed by circular frames and linear stingers with a thin aluminium skin. This lightweight stiff structure efficiently transmits and radiates noise to the interior when excited by acoustic sources (i.e. propeller or jet noise), by aerodynamic sources (i.e. pressure fields produced by turbulent boundary layer air flow on the aircraft skin) and by structure borne paths (i.e. engine induced vibrations or airframe vibrations induced by airflow effects on the wings and landing gears during take off and landing manoeuvres).[1-3] Passive treatments, such as double wall constructions with sound absorption treatments in the air gap or damping and mass treatments on the skin of the fuselage, can be used to partially reduce these problems,[2,4,5] although they tend to be ineffective at low audio frequencies unless bulky and heavy treatments were to be used. Recent research work has shown that decentralized active vibration control with point force actuators provides an efficient solution to the low frequency sound radiation and transmission problems due to broad band random excitations, as for example, jet noise, turbulent boundary layer pressure fields or airframe structure borne noise due to aerodynamic excitations.[6]

At low frequency, the sound radiation by a lightly damped trim panel is characterised by well separated resonances of the low order modes of the panel.[7] Thus, steady state broad band sound radiation can be reduced by enhancing the damping properties of the trim panel, which can be effectively achieved by velocity feedback control systems.[8] If ideal point force actuators and velocity sensors are used, then collocated velocity feedback is bound to be unconditionally stable.[9-11] In practice, force actuators are constructed with an electrodynamic actuator that reacts off a proof mass. This type of actuator produces a constant force in phase with the driving voltage signal above the fundamental resonance frequency of the resiliently mounted mass.[12] In contrast, at frequencies below the fundamental resonance frequency of the resiliently mounted mass, the force produced by the actuator tends to decrease in amplitude and shift to -180^{o} as the frequency goes down. Thus, the desired active damping action of the feedback control loop is produced only at frequencies above the fundamental resonance of the actuator. In contrast, below resonance, negative damping is produced which would enhance the resonant response and sound radiation of the panel and may even lead to instability.

This report introduces the stability and control performance tests carried out on a BOMBARDIER Dash-8 Q400 fuselage section with trim panel which is equipped with five decentralised velocity feedback control units for the reduction of vibration and sound radiation. Section 2 provides a short description of the fuselage section and the modular feedback control units. Section 3 describes the experimental setup and tests carried out to assess the effectiveness of the control units. Finally, section 5 presents the experimental results for the response of the fuselage section in three cases: a) when there are no control units on the trim panel; b) when the trim panel is equipped with open loop control units and c) when the trim panel is equipped with closed loop control units.

2. FUSELAGE SECTION AND CONTROL SYSTEM TEST RIG

The dimensions of the fuselage section considered in this report have been chosen in such a way as to carry out experimental measurements that could be representative of the sound transmission and radiation properties in a medium size propeller aircraft at low audio frequencies where active control is particularly effective.

The principal components of the decentralised control units mounted on the trim panel are also introduced. In particular the design and response of the electrodynamic inertial actuator in the control units is described in detail.

2.1. Fuselage section

As shown in Figure 1a the fuselage section considered in this study is composed of an aluminium structure with two frames, 580 mm apart from each other, and five stringers, 124 mm apart from each other, on which leans the 1.6 mm thick aluminium skin of the aircraft. As shown in Figure 1b a curved rectangular trim panel, with surface 589 × 550 mm^2, made of a lightweight honeycomb material is connected to the frames via four elastic mounts. The air gap between the skin and trim panel is about 81 mm.

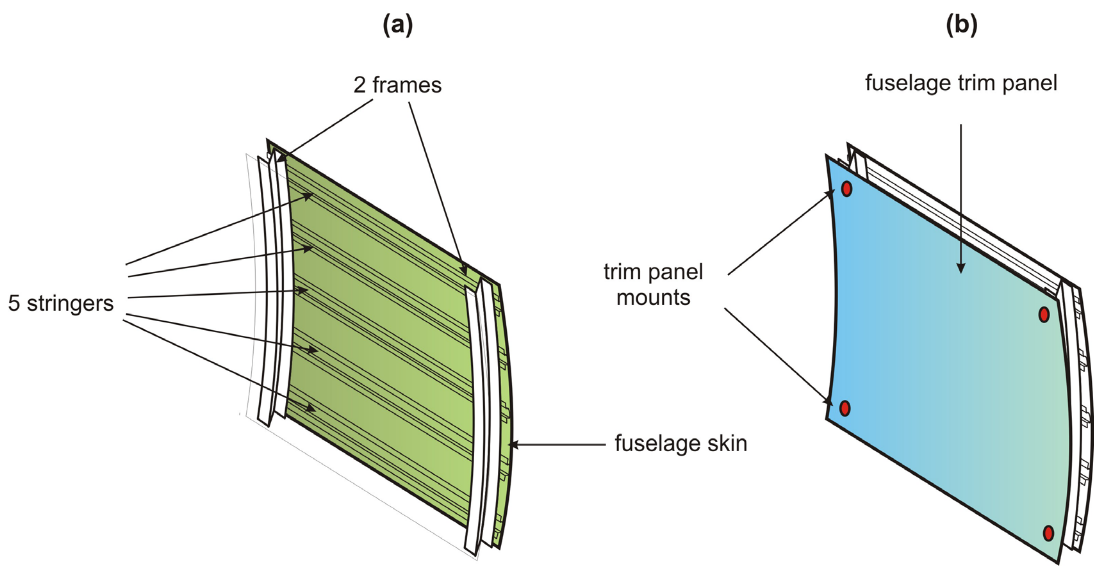

Fig. 1: Sketch of the fuselage section. (a) Green fuselage section composed of two frames and five stingers. (b) Trim panel fixed on four mounts.

The details for the dimensions and material properties of the frame structure, fuselage skin and interior trim panel are given in Figure 2 and Tables 1 and 2. Also the positions of the four mounts with respect to the trim panel are listed in Table 3.

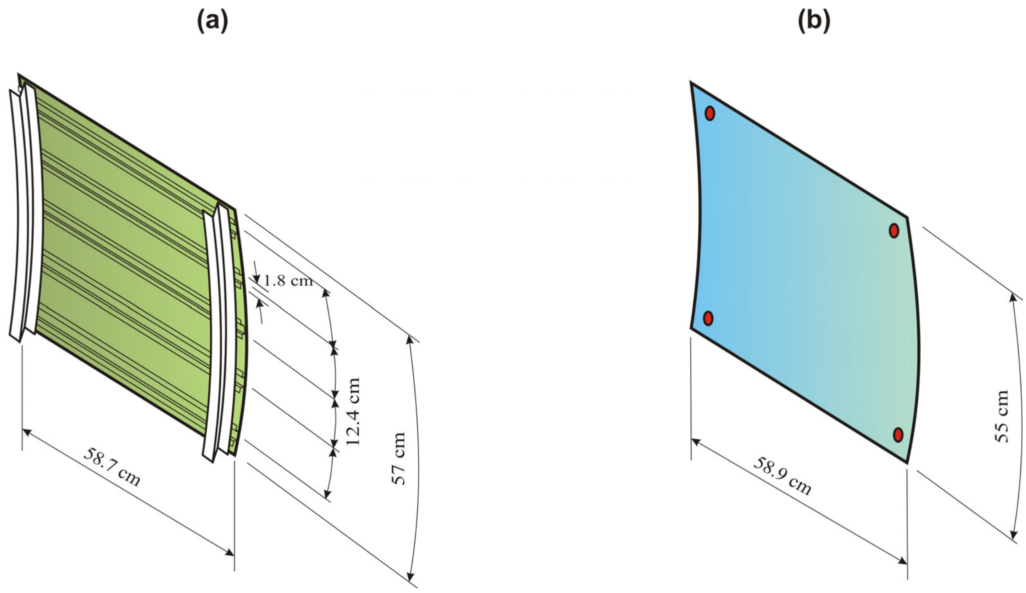

Fig. 2: Principal dimensions of the fuselage double wall.

Table 1: Material properties of the fuselage skin and frames, i.e. aluminium

Parameter	Value
Mass density	$\rho = 2720\ \mathrm{Kg/m^3}$
Young's modulus	$E = 7.1 \times 10^{10}\ \mathrm{N/m^2}$
Poisson ratio	$\nu = 0.33$
Damping loss factor	$\eta = 0.02$
Dimensions of the curved skin	$l_x \times l_y = 589 \times 550$ mm
Thickness of the skin	$h = 1.6$ mm
Thickness of the frame profile	$h_f = 2.5$ mm
Thickness of the stringers profiles	$h_s = 23$ mm

Table 2: Material properties of the honeycomb trim panel.

Parameter	Value
Dimensions	$l_x \times l_y = 589 \times 550$ mm
Faceplates thickness	$h_{fp} = 0.9$ mm
Core thickness	$h_{co} = 6$ mm
Total thickness (core and face plates)	$h_{ho} = 7.8$ mm
Smeared Mass density	$\rho = 2720\ \mathrm{Kg/m^3}$
Smeared Young's modulus	$E = 7.1 \times 10^{10}\ \mathrm{N/m^2}$
Poisson ratio	$\nu = 0.33$
Damping loss factor	$\eta = 0.02$

Table 3: Position of the mounts

Parameter	Value
Position of mount 1	x_{c1}, y_{c1} = 0.057m, 0.030m
Position of mount 2	x_{c2}, y_{c2} = 0.565m, 0.030m
Position of mount 3	x_{c3}, y_{c3} = 0.057m, 0.507m
Position of mount 4	x_{c4}, y_{c4} = 0.565m, 0.507m

2.2. Active Damping Control Unit

In this study, the fuselage section has been equipped with five decentralised control units. As shown in Figure 3, the control units are composed of an electromagnetic inertial actuator with an accelerometer sensor located at the centre of the actuator footprint. The accelerometer signal is first integrated in order to obtain the velocity at the base of the actuator. The velocity signal is then passed through a high pass filter with corner frequency around 10 Hz which is used for DC decoupling. Finally the signal is amplified with a voltage amplifier and then fedback back to the electromechanical inertial actuator. The inertial actuator generates on the structure a point force, which is therefore proportional to the opposite of the velocity at the actuator base so that it produces a damping action.

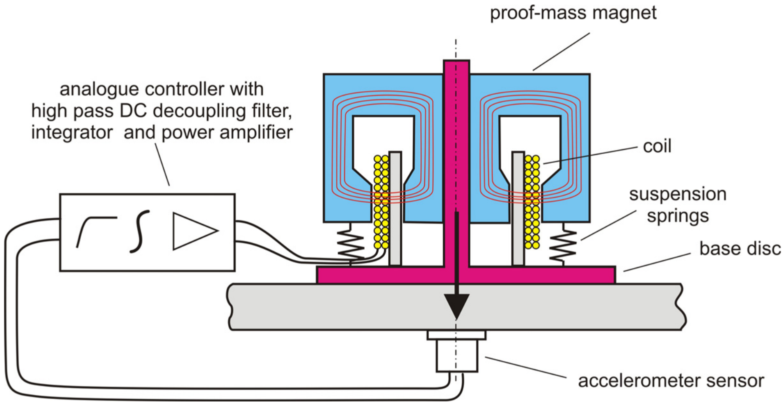

Fig. 3 Sketch of the active damping control unit composed of a proof mass electromagnetic actuator, an accelerometer sensor and an analogue controller.

The small scale electrodynamic inertial actuator used for this study is shown in Figure 4. As schematically shown in Figure 3, this actuator is composed of a base disc with a cylindrical former on which the coil is wound. The proof mass is formed by a magnetic core cylinder and an outer ferromagnetic ring. The proof mass is mounted on three springs and a vertical bushing, which forces the magnet to oscillate in the axial direction.

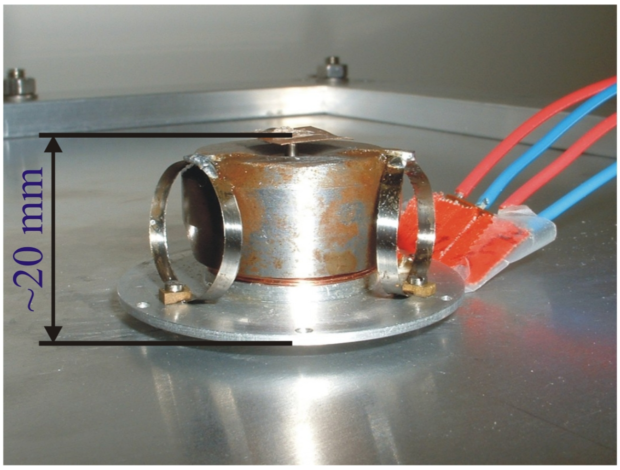

Fig. 4: Photo of the electrodynamic proof mass actuator.

As shown in Figure 4, the three springs are made up of small circular rings which guarantee a relatively larger stiffness in the transverse direction than in the axial direction. In this way the fundamental axial natural frequency of the proof mass actuator can be kept rather low with a good transverse guiding which prevents non linear effects due to stick slip friction on the axial bushing. As shown in Figure 3, the cross section of the proof mass is shaped in such a way as to have a magnetic circuit that generates a field oriented in the direction orthogonal to the coil winding. In this way a current flow through the coil produces the reactive axial force between the coil and the proof mass. The details of the design of the circular springs and coil-magnet transducers are presented by Paulitsch.[13] The physical and geometrical properties of the actuator are summarised in Table 4.

Table 4: Geometry and physical parameters of the actuator.

Parameter	Value
Proof mass diameter	24 mm
Proof mass height	12 mm
Magnet diameter	18 mm
Magnet height	9.3 mm
Base disk diameter	38 mm
Base disk thickness	1 mm
Housing and base disk mass	$M_b = 8$ g
Proof mass	$M_a = 22$ g
Suspension system stiffness	$K_a = 347.4$ N/m
Suspension system damping	$C_a = 3.3$ N/ms^{-1}
Fundamental natural frequency	$f_a = 20$ Hz
Voice coil coefficient	$\psi = 2.6$ N/A

2.3. Fuselage Section with Five Active Damping Control Units

As shown in Figure 5 and listed in Table 5, in order to generate a substantial active damping action, the trim panel has been equipped with five control units arranged on the centre and along the diagonals of the panel.

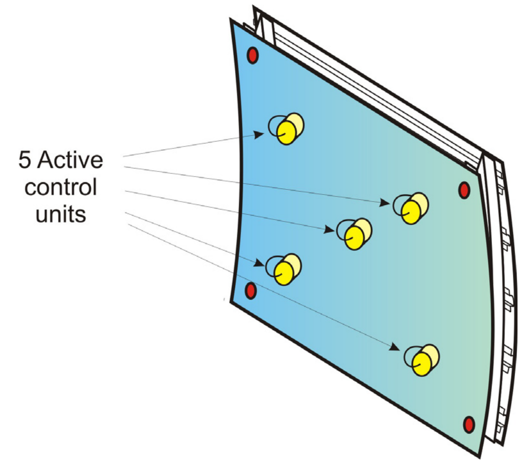

Fig. 5: Fuselage section with the five control units.

As shown in Figures 6 , 7 and 8, the five control units have been attached on the interior side of the trim panel so that they are enclosed in the air gap between the fuselage skin and trim panel. The accelerometer sensors have been located in correspondence to the centres of the footprint of the actuators on the radiating side of the trim panel. The five analogue controllers have been constructed using off the shelf components without aiming to miniaturise and package them with the actuator and sensor transducers. The rack with the five controllers can be seen on the bottom left hand side of Figure 7.

Table 5: Position of the feedback control units.

Parameter	Value
Position of the primary excitation	x_p, y_p = 0.085m , 0.096m
Position of control system 1	x_{c1}, y_{c1} = 0.160m, 0.295m
Position of control system 2	x_{c2}, y_{c2} = 0.430m, 0.295m
Position of control system 3	x_{c3}, y_{c3} = 0.160m, 0.150m
Position of control system 4	x_{c4}, y_{c4} = 0.430m, 0.150m
Position of control system 5	x_{c5}, y_{c5} = 0.295m, 0.275m

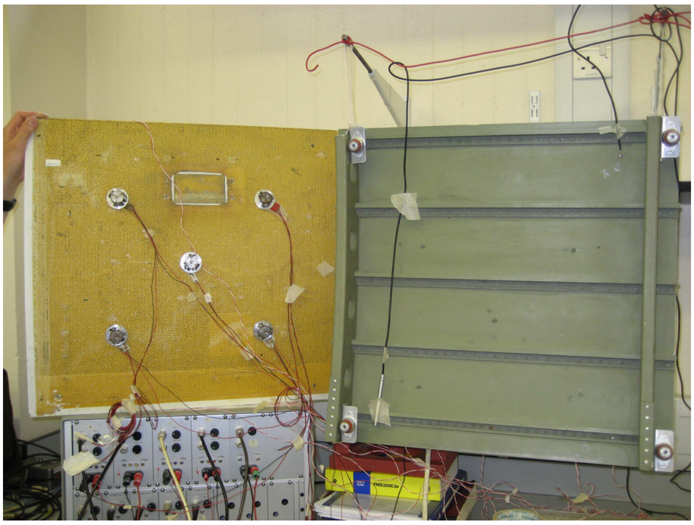

Fig. 6: Front view of the fuselage section and trim panel with five control actuators bonded on the interior side.

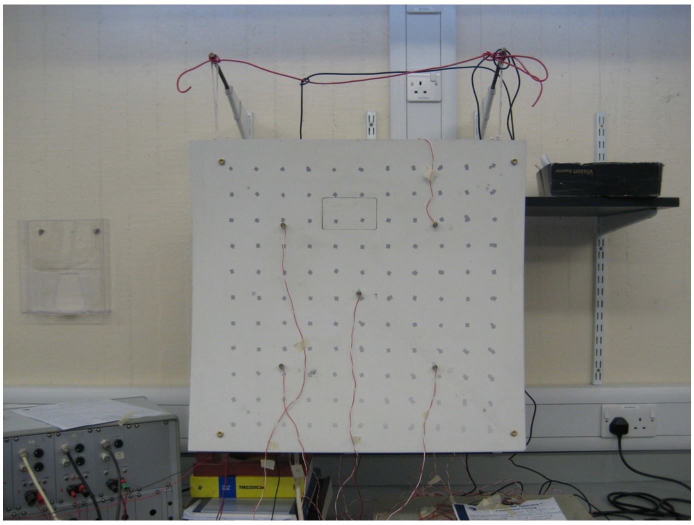

Fig. 7: Front view of the fuselage section and trim panel with five accelerometers bonded in correspondence to the centre of the actuators footprints.

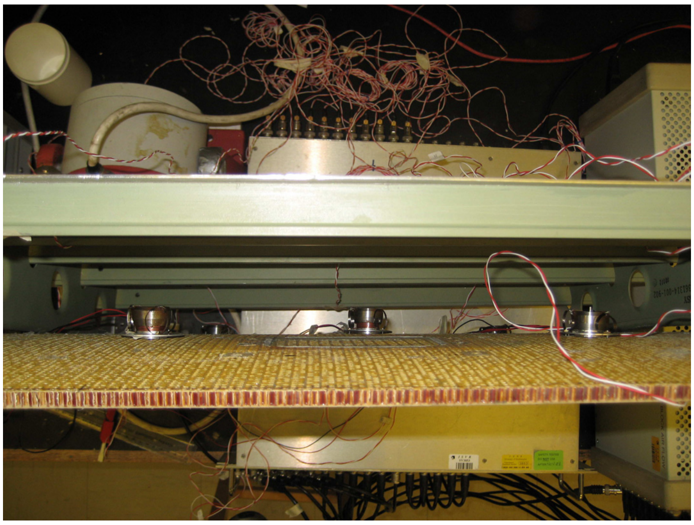

Fig. 8: Top view of the fuselage section and trim panel with five actuators bonded on the interior side.

2.4. Experimental tests

In this report preliminary tests are presented concerning the response of the double panel system without and with open loop and closed loop control units. For simplicity the experiments have been carried out with the fuselage section suspended by two bandages fastened at the top end of the two frames as shown in Figure 9a. The response of the fuselage section has been measured with a scanning laser vibrometer. As shown in Figure 9b, the fuselage has been excited by a point force located near the bottom left corner at position x_p , y_p = 0.565 m , 0.507 m.

Two types of experimental results have been produced: first, the spectrum of the spatially averaged response of the trim panel per unit primary excitation and second, the vibration field of the trim panel per unit excitation at a given frequency. Despite the simplicity of these initial experiments, they provide a good estimate of the response and nearfield sound radiation of the trim panel when most of the natural modes of the fuselage skin section are excited. The spectrum of the sound transmission is likely to be characterised by fewer resonances since the far field sound radiation of some odd – odd modes is attenuated by low radiation efficiency properties. Similarly the excitation produced by acoustic plane waves or by random acoustic fields or pressure fields generated by Turbulent Boundary Layer air flows is likely to unevenly excite the low frequency modes. Nevertheless the experiments presented in the following sections should provide a good account of the response and sound radiation of the trim panel without and with open and closed loop control units.

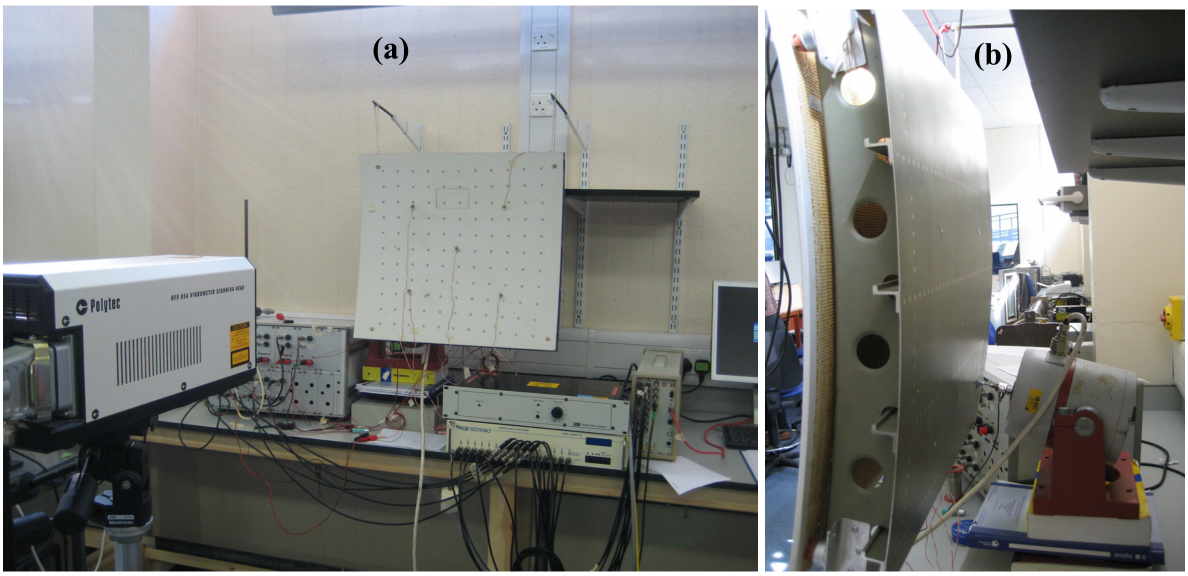

Fig. 9: Measurement setup with laser vibrometer and shaker primary actuator. (a) Front view, (b) lateral view.

3. STABILITY OF THE CONTROL SYSTEM

When dual and collocated sensor–actuator pairs are used, decentralised velocity feedback control is bound to be unconditionally stable.[9-11] In practice, the duality and collocation properties are possible only within certain limits whatever the sensor and actuator pair is. For instance, considering the inertial proof mass actuator and accelerometer sensor arrangement under study, the actuator produces a point force excitation in phase with the driving signal only above its fundamental resonance frequency and up to about 3 kHz.[12] Below the fundamental resonance frequency, the dynamics of the suspended mass produces a force with opposite phase to the driving signal. This 180° phase mismatch disrupts the duality between the actuation force and the velocity signal measured at the base of the actuator. For this reason, the actuator has been designed with a very low resonance frequency. Above 3 kHz the inductance of the coil motor produces a constant phase lag which also disrupts the duality property. For this reason a low inductance coil-magnet linear motor should be used within the limitations imposed by the required actuating force. The accelerometer sensor may also disrupt the duality property.[12] In fact above its characteristic resonance frequency, the output signal is proportional to displacement rather than acceleration. Finally the controller also introduces phase lag that contributes to disrupt the stability of the feedback loop.[12] These intrinsic instability problems worsen when multiple feedback loops are implemented. For instance, the cross talking effects between neighbouring actuators tend to emphasise the low frequency stability problem linked to the fundamental resonance of the actuator.[14]

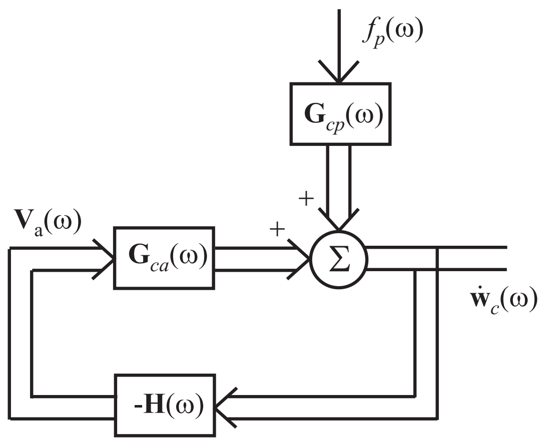

Fig. 10: Block diagram of the multichannel feedback control system implemented on the trim panel

In view of these considerations, it is of great importance to assess the stability of the control system before closing the feedback control loops. The stability of a single feedback control unit can be assessed with the Nyquist criterion,[15] which states that, provided the controller is stable, the feedback loop is bound to be stable provided the locus of the sensor–actuator FRF does not encircle the Nyquist instability point (-1,j0). However, when multiple loops are implemented simultaneously, the generalised Nyquist stability criterion[16] should be used. The open and closed loop response at the error sensor of the decentralised feedback loops can be modelled with the block diagram shown in Figure 9 where $\mathbf{G}_{ca}$ represent the 5×5 matrix of frequency response functions between the sensors and actuators and **H** is a diagonal matrix with the feedback control gains that are assumed to be all the same. In this case, the generalised Nyquist stability criterion states that, assuming that both the plant and controller are individually stable, a multichannel feedback system is bound to be stable provided the locus of $\det[\mathbf{I} + \mathbf{G}_{ca}\mathbf{H}] = 0$ does not encircle the instability point $(0, j0)$ as ω varies from $-\infty$ to $+\infty$.[6] Thus, for the case of decentralised control with the same control gains for all feedback loops, so that **H** is a diagonal matrix, the stability of the control loop can be assessed by considering the fully populated matrix of frequency response functions (FRFs) between the five control velocities and the five input current signals to the controller driving each actuator. Moreover, the determinant of a matrix is the product of its eigenvalues;[16] that is $\det[\mathbf{I} + \mathbf{G}_{ca}\mathbf{H}] = (1 + g\lambda_1)(1 + g\lambda_2)\cdots(1 + g\lambda_5)$, where $\lambda_i(\omega)$ is the i-th eigenvalue of $\mathbf{G}_{ca}\mathbf{H}$. Thus the stability analysis of the five channel control system can be implemented with reference to the polar plots of the five eigenvalues of $\mathbf{G}_{ca}\mathbf{H}$. In this case, in order to ensure the system is stable, the five loci should not encircle the instability point (-1,j0) as ω varies from $-\infty$ to $+\infty$.

Figure 10 shows the amplitude and phase plots for the Frequency Response Functions between the five sensors and five actuators. The diagonal plots provide the FRFs for each sensor–actuator pair. Thus the FRFs in the diagonal plots of Figure 10 can be used to assess the stability of individual feedback loops. The phase plots show that the phase of the sensor–actuator FRFs exceed $+90^{o}$ at low frequencies, around the fundamental resonance of the inertial actuator, and -90^{o} at higher frequencies where the inductance effect of the coil produces a constant phase lag. As a result the FRFs are not positive real and thus may encircle the Nyquist critical point. Indeed, at low frequency the phase goes up to $+270^{o}$ and at higher frequencies it exceeds -360^{o}.

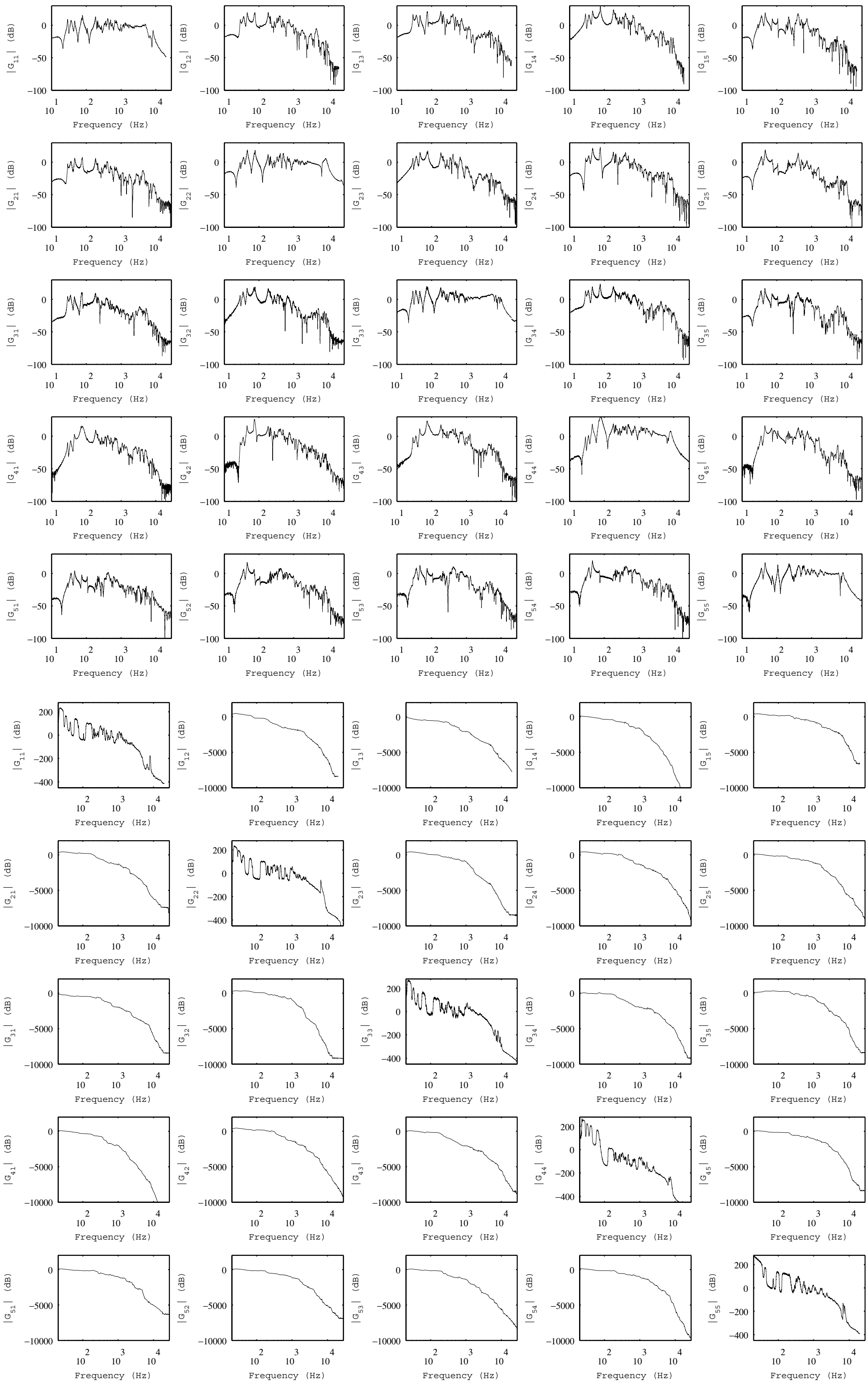

Fig. 11: Amplitude and phase of the measured FRFs between the five error sensors and five inputs to the controllers driving the actuators.

The low frequency problem is quite important since, as can be noticed in the diagonal plots, the amplitudes of the FRFs are relatively high at low frequencies and thus little gain margin is likely to be left unless the fundamental resonance of the actuator is well damped and kept at low frequency.

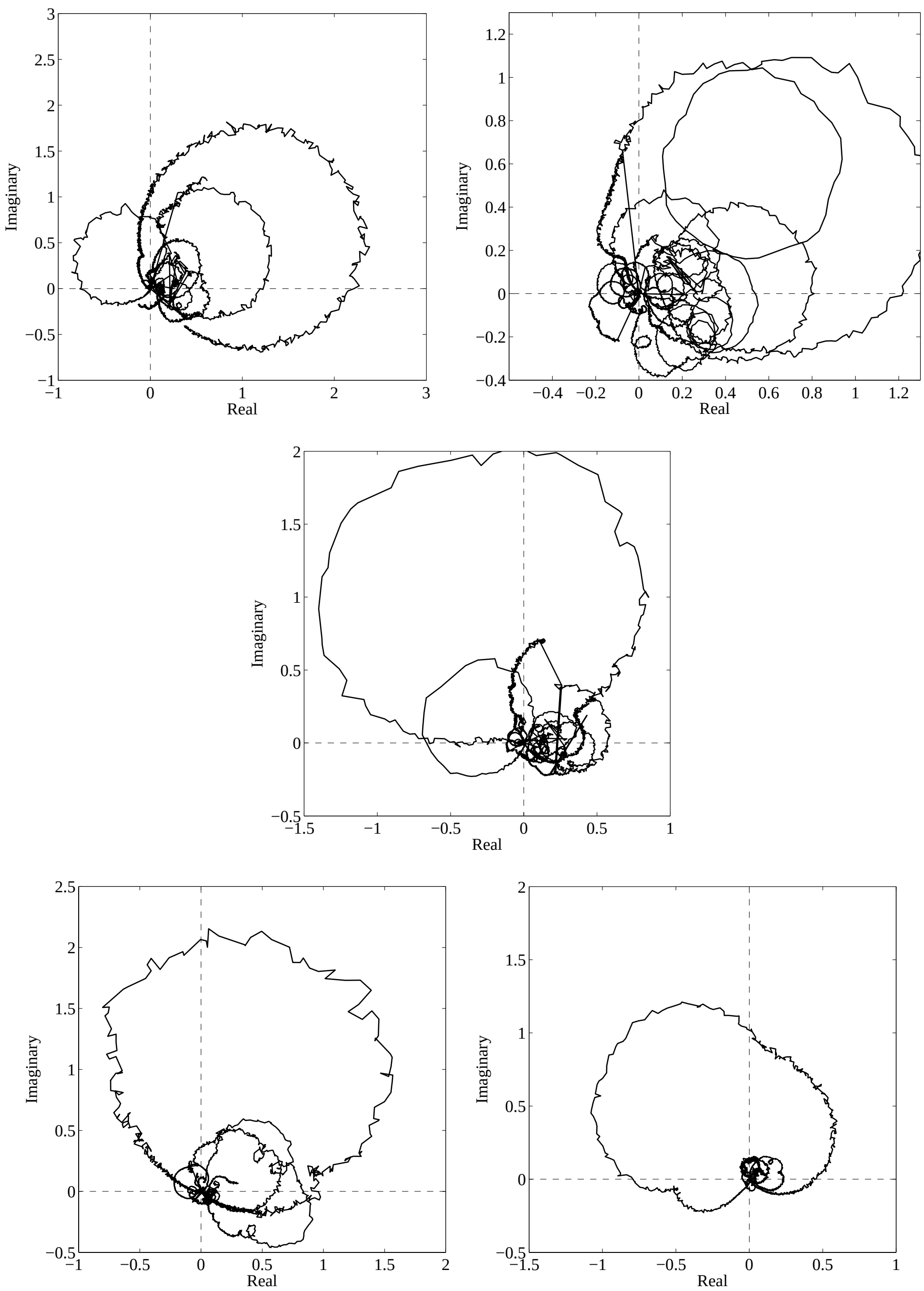

Fig. 12: Block diagram of the multichannel feedback control system implemented on the trim panel

The off diagonal plots with the amplitudes of the cross FRFs between non collocated sensors and actuators are comparable to those of the self FRFs between collocated sensors and actuators. This suggests that there is a significant cross talking between the five feedback control loops which should also affect the stability when the five control units are activated simultaneously. Indeed the five plots in Figure 12 with the eigenvalues of the $\mathbf{G}_{ca}\mathbf{H}$ confirm that only a limited range of control gains can be implemented otherwise the set of five control loops would go unstable.

4. EXPERIMENTAL TESTS

In this section the frequency response function (FRF) of the transverse response of the trim panel per unit excitation of the shaker primary force excitation is investigated in three cases:

1) trim panel without control units;
2) trim panel with open loop control units and
3) trim panel with closed loop control units.

For each case the spatially average response per unit excitation is plotted in a frequency range between 10 and 600 Hz. Comparison of the plots for the three cases will give an indication of the passive and active effects produced by the five control units at low audio frequencies. Also the spatial response at specific resonance frequencies has been plotted in order to investigate how the passive and active effects of the control units modify the response of the trim panel.

4.1. Response of Trim Panel without Control Units

Figure 13 shows the spatially averaged FRF of the transverse response of the panel per unit force exerted by the shaker in a frequency range between 10 and 600 Hz. The spectrum is characterised by sharp peaks due to the resonant response of the fuselage section and trim panel. The spectrum shows two clusters of resonances. The first is composed of about six resonances between 10 and 106 Hz. These resonances are very lightly damped and produce large responses. The second cluster is composed of about 10 resonances, between 196 and 422 Hz, which are also lightly damped although their amplitudes are about 7 dB lower than those of the first cluster of resonances. At higher frequencies above 500 Hz there are wide band peaks which may be generated by combinations of neighbourhood resonant modes of the fuselage structure, fuselage skin, trim panel and air cavity. The plots with the spatial response of the trim panel at the first 12 resonance frequencies shown in Figures 14 and 15, show that the cluster of resonances between 15 and 106 Hz are controlled by mode shapes characterised by either rigid body motion or first mode order flexural deformations of the trim panel. The second cluster of resonances between 196 and 422 Hz are instead controlled by bending mode shapes of the trim panel pinned at the four mounting positions.

The experimental work presented in this section has shown that, at low audio frequencies, the response of the trim panel is characterised by lightly damped resonances which are clustered in two principal groups at low frequencies. The modular active damping control units described in Section 3 should effectively control these resonances.

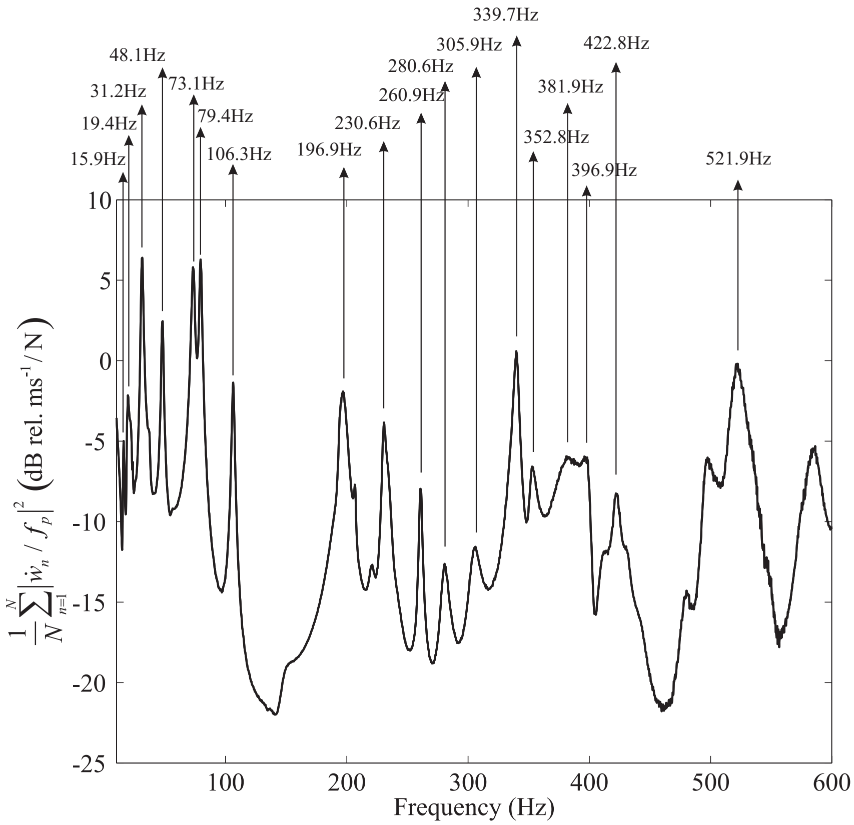

Fig. 13: Spatially averaged FRF of the trim panel without control units per unit force excitation.

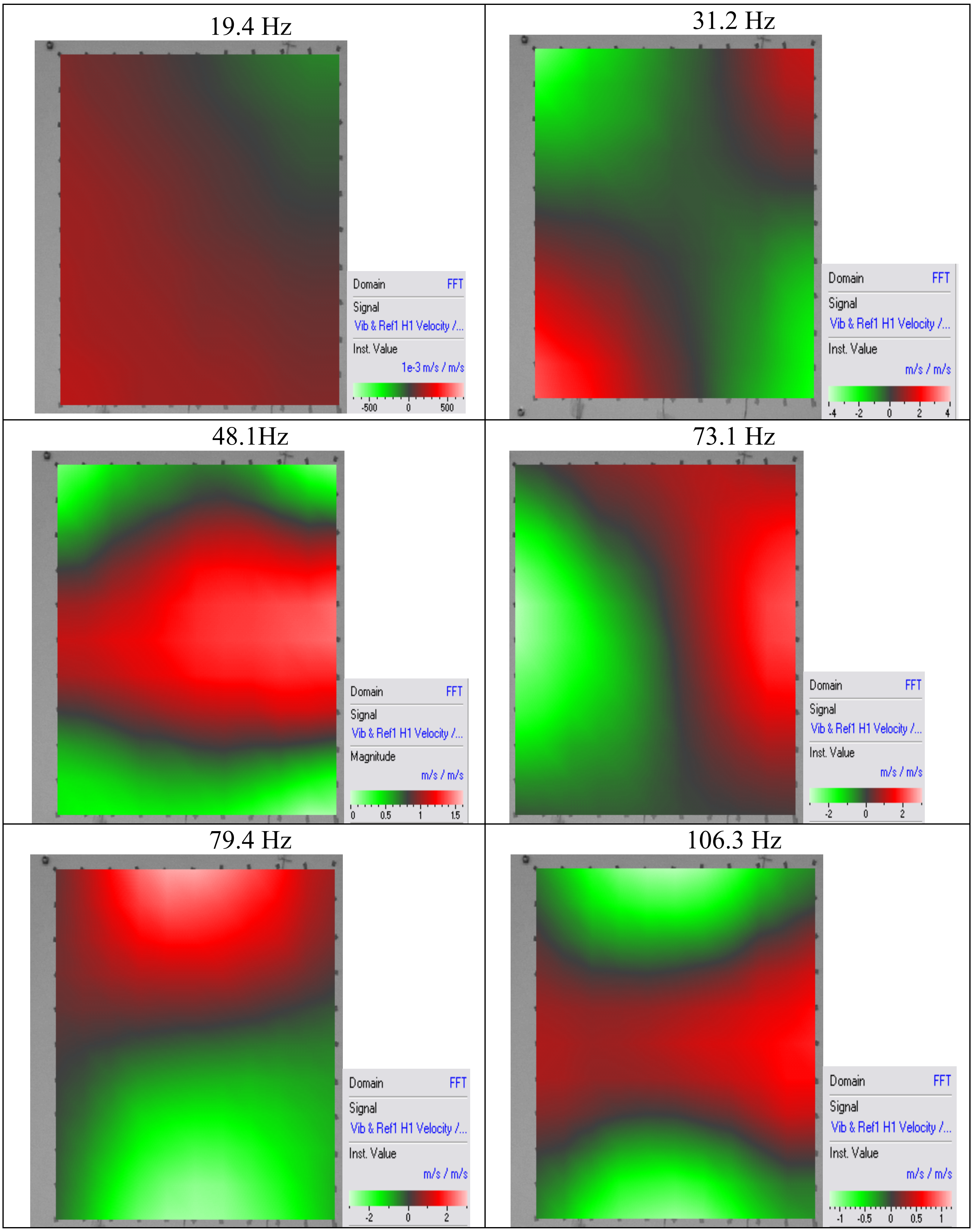

Fig. 14: Responses of the trim panel without control units at resonance frequencies.

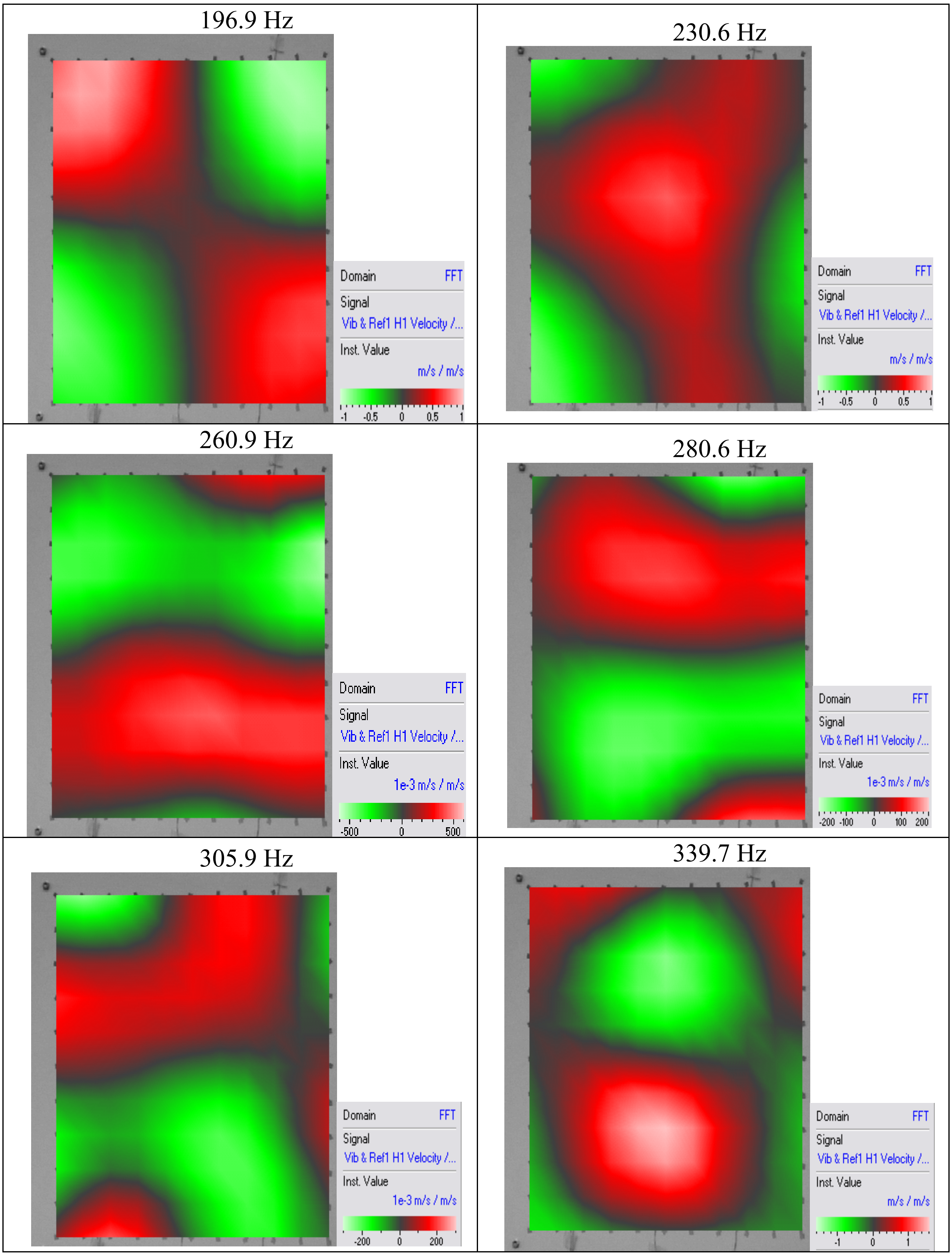

Fig. 15: Responses of the trim panel without control units at resonance frequencies.

4.2. Response of Trim Panel with Open Loop Control Units

Figure 16 shows the spatially averaged FRF of the transverse response of the panel without (solid black line) and with (dashed blue line) open loop control units per unit force exerted by the shaker in a frequency range between 10 and 600 Hz. The open loop control units have little effect on the first cluster of resonance frequencies. They slightly shift the resonances to lower frequencies indicating a mass effect. However, for the second cluster of resonances, the five open loop control units produce a reduction of vibration up to 7 dB except for the resonance at 260.9 Hz. This is due to the fact that, above the fundamental resonance of the actuator, the suspended mass acts as an inertial reference. As a result the vibration of the coil in the annular cavity of the seismic mass is equivalent to a dash pot damper that produces sky hook damping. Also, eddy current effects are likely to occur, which also produce dissipative effects. The passive effect of the open loop control unit becomes even more significant at higher frequencies above 500 Hz. Probably, together with the sky hook passive damping effect of the actuator, there is also a mass effect of the components of the control units firmly attached to the trim panel, i.e. base disk and coil of the actuator, part of the springs, accelerometer sensor, wiring. This effect is particularly important around the wide band resonance peak at 521.9 Hz where the response of the panel is reduced by about 8 dB.

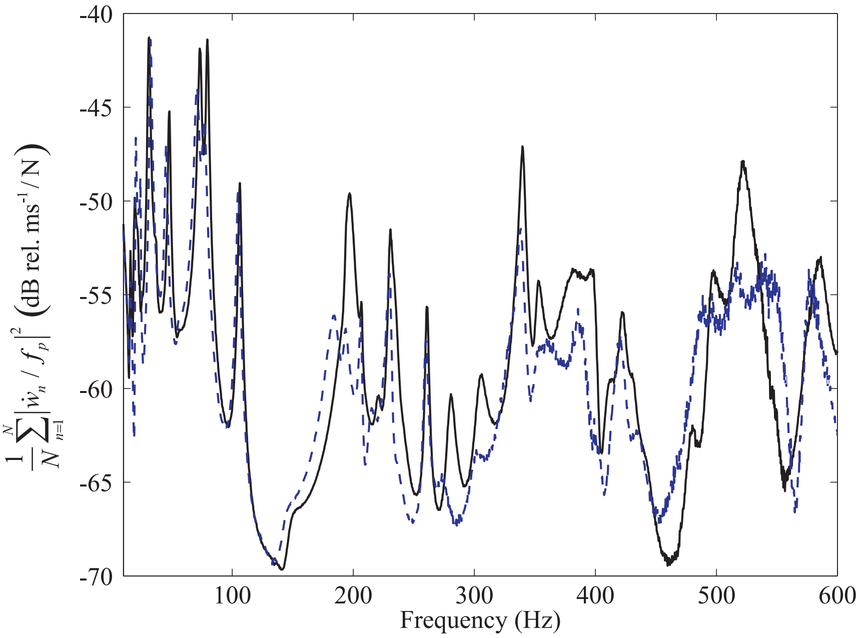

Fig. 16: Spatially averaged response of the trim panel per unit force excitation. Solid-black line without control units, dashed-blue line with open loop control units.

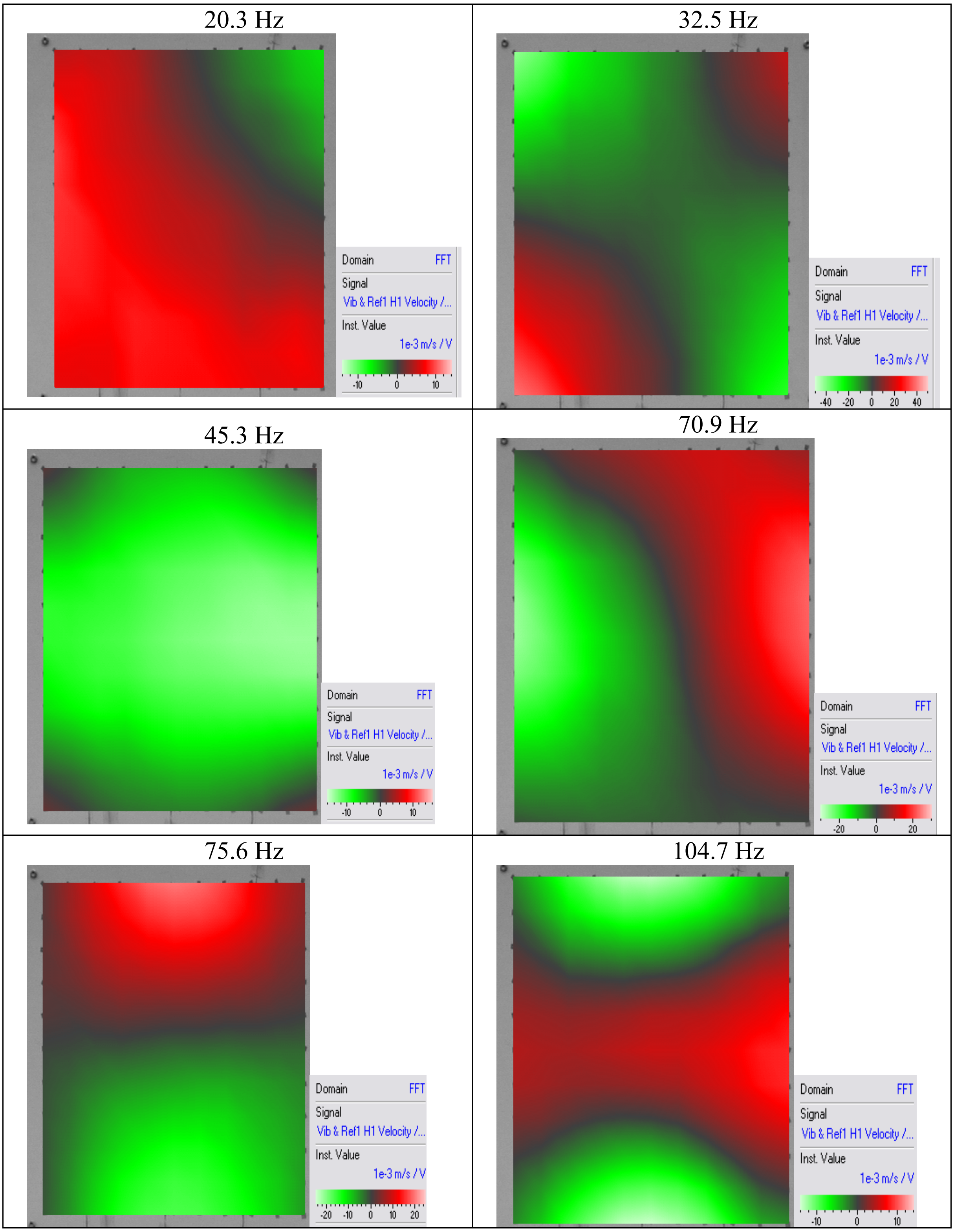

Fig. 17: Responses of the trim panel with open loop control units at resonance frequencies.

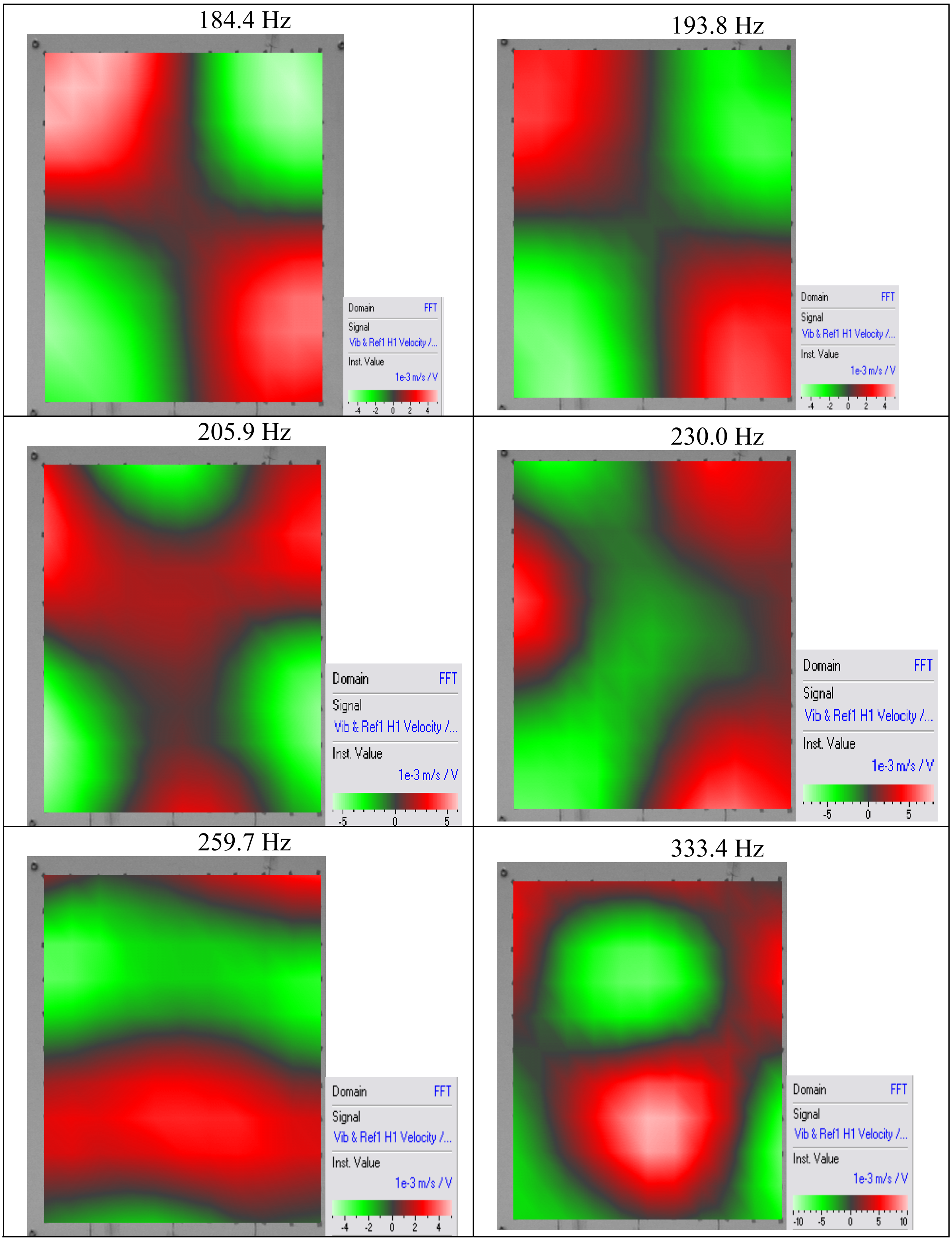

Fig. 18: Responses of the trim panel with open loop control units at resonance frequencies.

Comparing Figures 17 and 14 confirms that the spatial responses of the first six resonances of the trim panel are barely modified by the five control units. However, comparing Figures 18 and 15, highlights the fact that the control units have modified the response of quite a few resonances in the second cluster between 196 and 422 Hz.

4.3. Response of Trim Panel with Closed Loop Control Units

Figure 19 shows the spatially averaged FRF of the transverse response of the panel without control units (solid black line), with open loop control units (dashed blue line) and with closed loop control units (dotted red line) per unit force exerted by the shaker in a frequency range between 10 and 600 Hz. The closed loop control units have little effect on the first three resonance frequencies up to 31.2 Hz. However, comparing the open and closed loop results, they produce about 5 to 7 dB vibration reductions of the first cluster of resonances 48.1, 73.1 and 79.4 Hz. Also, good vibration reductions are achieved for some resonance peaks of the second clusters such as, for example, around the peak at 196.7 Hz. At higher frequencies the five control units produces about 3 to 5 dB reductions, particularly between 340 and 390 Hz and between 450 and 550 Hz.

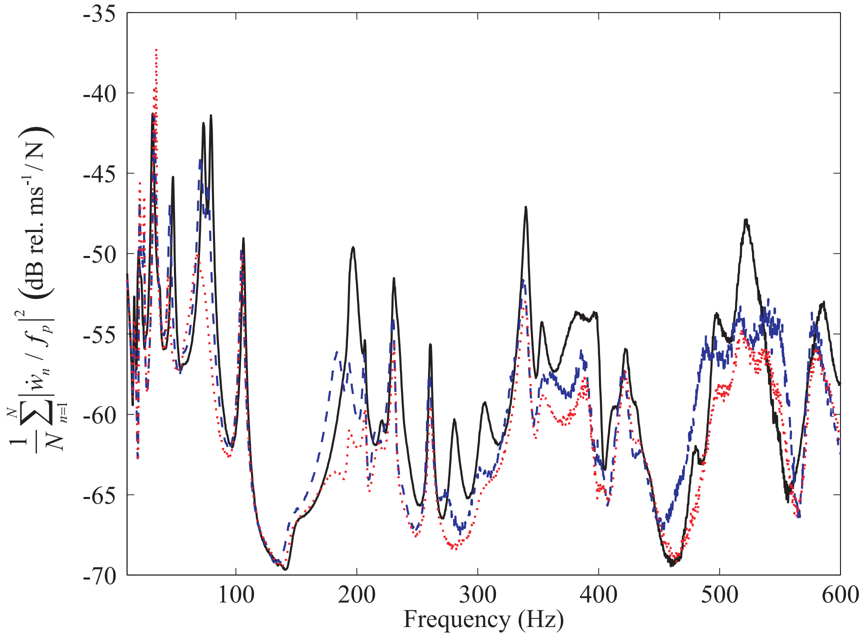

Fig. 19: Spatially averaged response of the trim panel per unit force excitation. Solid-black line without control units, dashed-blue line with open loop control units, dotted-red line with closed loop control units.

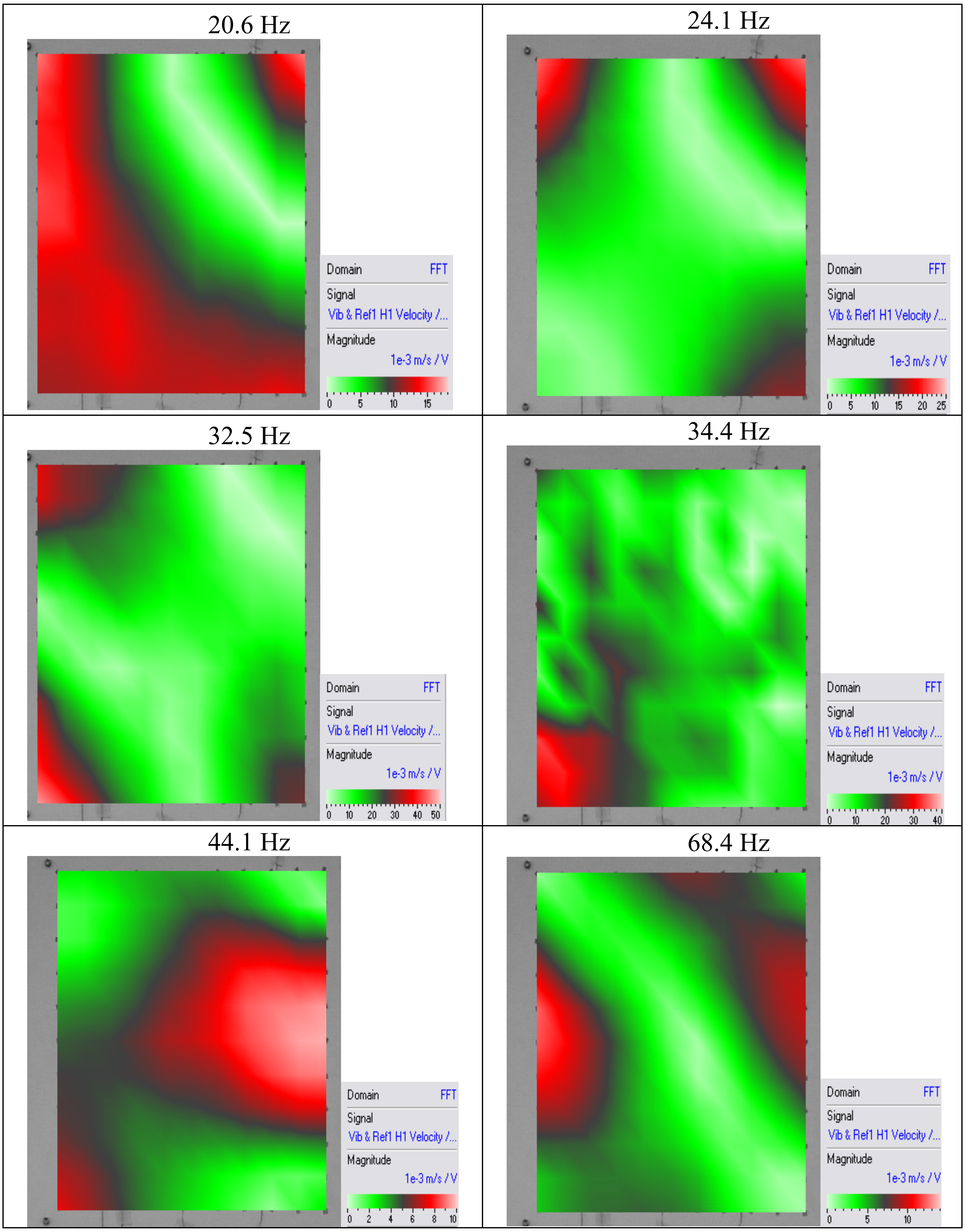

Fig. 20: Responses of the trim panel with closed loop control units at resonance frequencies.

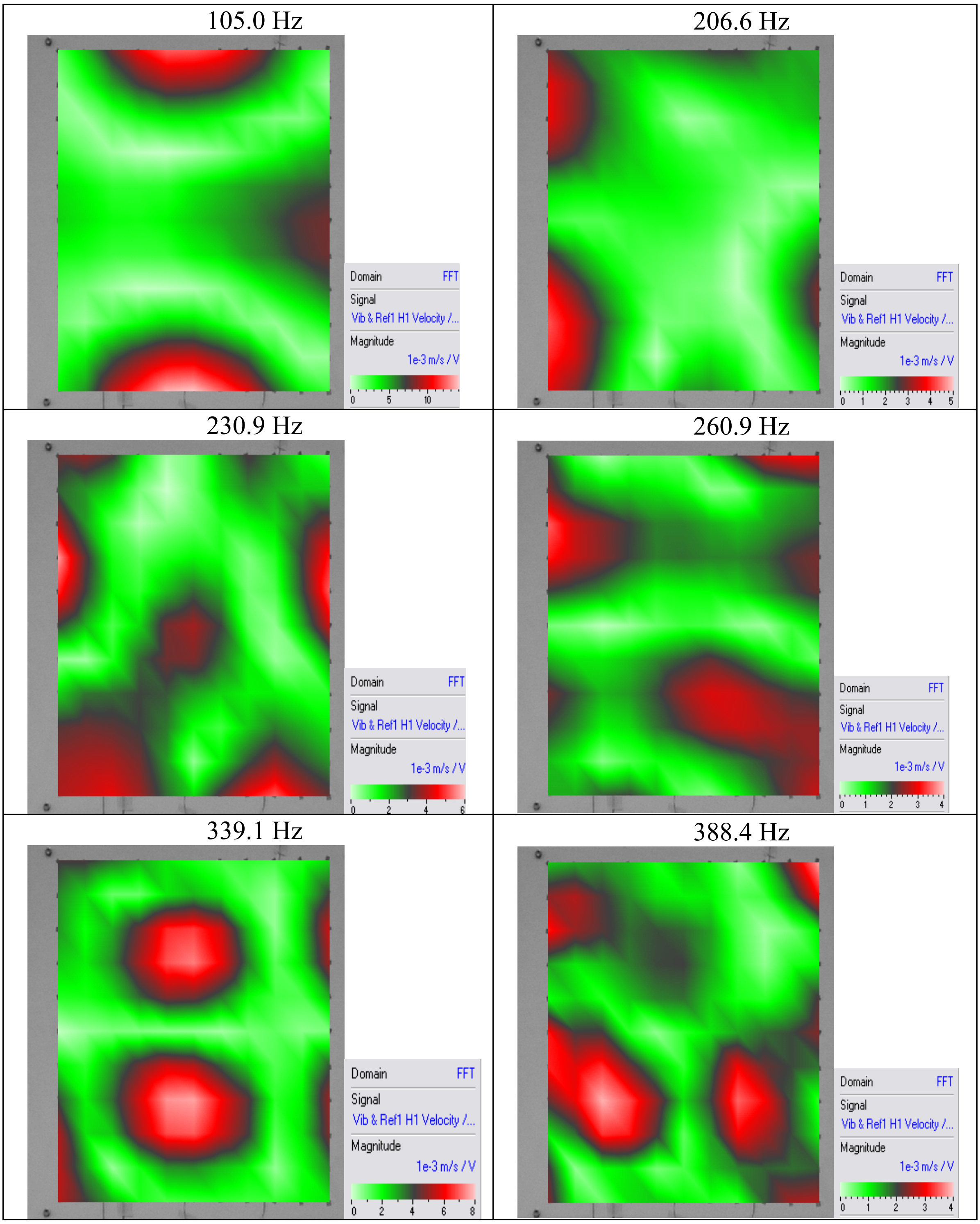

Fig. 21: Responses of the trim panel with closed loop control units at resonance frequencies.

Figures 20 and 21 show that the five closed loop control units have an important effect on the spatial response of the trim panel. The responses are no longer characterised by well defined mode shapes of the trim panel, which indicates that indeed the passive and active damping action of the control units has heavily reduced the vibration contribution of the resonant modes.

In summary, the combination of passive and active control effects generated by the five control units produces an overall reduction of vibration between 4 dB and 15 dB in the frequency range 30 to 520 Hz.

5. CONCLUSIONS

This report presents the experimental work carried out to implement decentralised velocity feedback control on a fuselage section of a Bombardier Dash-8 Q400 aircraft. Five velocity feedback control units have been mounted on the trim panel of the fuselage section in order to reduce its response and thus sound transmission and radiation. The velocity feedback control units are composed of an electromagnetic inertial actuator with an accelerometer sensor located at the centre of the actuator footprint. In order to implement velocity feedback, the accelerometer signal is first integrated, amplified and then fed back to the electromechanical inertial actuator. In this way the point force generated by the electromagnetic actuator on the trim panel is proportional to the opposite of the velocity at the actuator base and thus it produces a damping action that reduces its response and sound radiation.

The effects of the control systems have been assessed with reference to the response of the trim panel to a point force excitation exerted by a shaker on the skin of the fuselage section. The principal outcomes of this study can be summarised in the following points.

1) At low audio frequencies, the response of the trim panel is characterised by clusters of lightly damped resonances due to rigid body modes or low modal order flexible modes of the trim panel.
2) At higher frequencies the response of the trim panel is characterised by wide band resonant peaks which are due to the neighbouring resonant modes of the various components of the fuselage section, i.e. the frames and stringers, the fuselage skin, the trim panel and the air cavity between the skin and panel structures.

3) The five control units produce significant passive effects on the response of the panel. In particular, at low audio effects, the inertial mass and coil system form a dash pot system that effectively produces passive damping effects. Also, at higher frequencies, the components of the control units rigidly attached to the trim panel produce a mass effect. The superposition of the two effects can bring down the response of the panel by as much as 8dB at some resonance frequencies.
4) The active damping action produced by the five control units further reduces the response of the trim panel at resonance frequencies of low order modes by another 5 to 7 dB.
5) The passive and active effects produced by the control units produce an overall reduction of vibration between 4 dB and 15 dB in the frequency range 30 to 520 Hz.

6. FUTURE WORK

The results presented in this report summarise the initial work carried out to test the effectiveness of decentralised velocity feedback control using inertial electrodynamic actuators built by ISVR PhD students. Future work is required to further develop the control system and also to better understand the dynamic response of the structure and thus identify the type of control action that should be implemented by the control units in order to obtain the best possible control performance. Future work would be of great interest in the following areas.

1. Theoretical and experimental analysis of the response of the fuselage section in order to understand the effects produced by
   - curved frame structure and skin panel
   - curved honeycomb trim panel fixed via four mounts
   - coupling between the skin and trim panel via structure (frame and mounts) and acoustic (air gap) paths
2. Analysis of the passive and active response of the trim panel with five control units when the fuselage skin and the trim panel is equipped with sound absorption blankets.

3. Implementation of sound radiation and sound transmission tests with reference to acoustic or random pressure fields (without control units, with open loop control units and with closed loop control units).
4. Development of suitable control units comprising accurately designed control actuators, miniaturised controllers and low cost MEMS accelerometer sensors.

AKNOWLEDGEMENTS

The work carried out by Cristóbal González Díaz was supported by a fellowship awarded by the Platform Grant "Structural Acoustics" programme, which is supported by the Engineering and Physical Sciences Council in the United Kingdom.

The authors would like to thank Mr Andrew Wareing from BOMBARDIER in Toronto who provided the fuselage section used in this study.

REFERENCES

[1] E. J. Richards and D. J. Mead (Editors) 1968, *Noise and Acoustic Fatigue in Aeronautics*, London John Wiley & Sons LTD

[2] J. S. Mixson and J. S. Wilby, "Interior Noise," in H. H. Hubbard *Aeroacoustics of Flight Vehicles, Theory and Practice* NASA Langley Research Center Hampton, Virginia, 1995, 271-335, Chapter 16.

[3] P. Gardonio, "Review of active techniques for aerospace vibro-acoustic control," *Journal of Aircraft* **39** (2): 206-214 (2002).

[4] F. J. Fahy, "Fundamentals of noise and vibration control," in F. J. Fahy and J. G. Walker *Fundamentals of noise and vibration* London: E & FN Spon, 1998, 225-309, Chapter 5.

[5] M. J. Brennan and N. S. Ferguson, "Vibration Control," in F. J. Fahy and J. G. Walker *Advanced applications in acoustics, noise and vibration* London: E & FN Spon, 2004, 530-580, Chapter 12.

[6] S. J. Elliott, P. Gardonio, T. C. Sors, and M. J. Brennan, "Active vibroacoustic control with multiple local feedback loops," *The Journal of the Acoustical Society of America* **111** (2): 908-915 (2002).

[7] F. J. Fahy and P. Gardonio. 2007. *Sound and structural vibration: radiation, transmission and response.* 2nd ed. London: Academic Press.

[8] C. Gonzalez Diaz, C. Paulitsch, and P. Gardonio, "Smart panel with active damping units. Implementation of decentralized control," *Journal of the Acoustical Society of America*, vol. 124, no. 2, pp. 898-910, 2008.

[9] A. Preumont. 2002. *Vibration control of active structures.* 2 ed. London: Kluwer Academic.

[10] M. J. Balas, "Direct velocity control of large space structures," *Journal of Guidance and Control* **2**: 252-253 (1979).

[11] V. Jayachandran and J. Q. Sun, "Unconditional stability domains of structural control systems using dual actuator-sensor pairs," *Journal of Sound and Vibration* **208** (1): 159-166 (1997).

[12] C. Gonzalez Diaz, C. Paulitsch, and P. Gardonio, "Active damping control unit using a small scale proof mass electrodynamic actuator," *Journal of the Acoustical Society of America*, vol. 124, no. 2, pp. 886-897, 2008.

[13] C. Paulitsch, "Vibration Control with electrodynamic actuators" (PhD Thesis, ISVR, University of Southampton, 2005).

[14] O. N. Baumann and S. J. Elliott, "The stability of decentralized multichannel velocity feedback controllers using inertial actuators," *The Journal of the Acoustical Society of America* **121** (1): 188-196 (2007).

[15] L. Meirovitch. 1990. *Dynamics and Control of Structures.* New York: John Wiley & Sons.

[16] S. J. Elliott. 2001. *Signal Processing for Active Control.* 1 ed. London: Academic Press.